Originally published in Engineering Structures 27 (2005) 1703-1712
with DOI: 10.1016/j.engstruct.2005.06.008
The final publication is available at http://www.sciencedirect.com

Static-cyclic tests on lightly reinforced concrete shear walls

Christian Greifenhagen [a,*], Pierino Lestuzzi [a]

[a] *Structural Engineering Institute (IS-IMAC)*

Ecole polytechnique fédérale de Lausanne, Switzerland

Abstract

This paper addresses strength and deformation capacity of squat reinforced concrete shear walls that are not designed for seismic actions. The seismic behavior of such walls is investigated in the framework of the study focussing on seismic evaluation of existing buildings. The results of a series of static-cyclic tests are presented and compared with data from the literature. The test series includes four lightly reinforced concrete shear walls in 1:3 scale of which horizontal reinforcement, axial force ratio, and concrete compressive strength is varied. Although brittle shear failure was predicted for the specimens, it is observed that lightly reinforced shear walls can have significant deformation capacity that is not affected by the ratio of horizontal reinforcement. It is also found that the flexural strength governs the observed strength in the tests while ultimate drift was limited by shear failure.

Key words: Reinforced concrete, shear walls, deformation capacity, low reinforcement ratio, static-cyclic tests, seismic evaluation, existing buildings

* Corresponding author. Postal address:

IMAC-IS-ENAC-EPFL, Station 18, CH-1015 Lausanne, Switzerland.

Tel.: +41 21 693 24 98; Fax: +41 21 693 47 48

Email address: christian.greifenhagen@epfl.ch (Christian Greifenhagen).

1 Introduction

Increased knowledge of seismic hazard in countries with moderate seismic exposure has necessitated the formulation of evaluation methods for structures that are not designed to withstand earthquake actions. In this context, experimental studies not only provide physical insight into force resisting mechanisms for development of models, but also the data to calibrate them, so that safe and efficient evaluation methods can be achieved. Since deformation based methods promise more realistic results than the force based methods, the former should be applied on existing buildings too [1]. Nevertheless, the characteristic details of existing buildings can lead to restricted deformation capacity which is investigated in this paper.

Reinforced concrete shear walls represent one of the most widespread bracing system for buildings. Post-earthquake reconnaissance missions report surprisingly good seismic behavior of structural wall buildings [2] while evaluation of existing buildings according to modern standards concludes often on insufficient safety margins [3]. An important number of existing buildings is stabilized by shear walls that are only designed for gravity loads, and not for lateral loads. Low reinforcement ratios, slenderness ratios less than 2.0, and inadequate seismic detailing characterize such walls. According to widely held views, squat reinforced concrete walls with low reinforcement ratios are susceptible to brittle shear failure restricting deformation capacity. Poor seismic performance is thus expected. Regarding the restricted deformation capacity that is associated with shear mechanisms, recent building codes prevent explicitly shear failure by the use of capacity design (EC8 [4], SIA 262 [5]).

This paper includes a database of shear wall tests. Criteria for the selection of the tests are configurations of existing buildings in Middle Europe and particularly in Switzerland [6]. Shear failure modes of squat walls [7] are discussed, and the relevance of these failure modes is shown for walls of rectangular cross-section that form the database. The study reveals that data from static-cyclic tests of walls prevalent in the described existing buildings were not yet available.

In this context, the paper reports a series of static-cyclic tests that is explicitly defined to investigate the deformation capacity of lightly reinforced concrete shear walls of existing buildings. The test series is a part of a research program that focuses on seismic evaluation of such structures. Variation of parameters, such as concrete compressive strength, axial force ratio, and horizontal reinforcement ratio, allowed both the identification of relevant failure modes and the observation of various failure modes that bound shear strength and ultimate drifts. Finally, the test results are compared with the database in terms of nominal shear stress ratio and drift.

2 Building configurations

Configurations of existing buildings in Switzerland are reported by Peter [6]. A typical existing building for which seismic evaluation would be required has between five and eight storeys. These buildings are usually stabilized by shear walls or by a mixed frame-wall system, and in-situ casted slabs of reinforced concrete. The shear walls are of 4 to 9 m length and 0.18 to 0.25 m in thickness. Prevalent cross-sections are rectangular or composed of rectangular cross-sections. Distributed horizontal and vertical reinforcement with ratios of

0.2 to 0.8 % is characteristic for such walls. In general, the reinforcing steel provides hardening ratios greater than or equal to 1.15 and uniform strains greater than 6 %. Finally, the concrete compressive strength meets values between 20 and 50 MPa.

3 Failure modes

Failure modes describe the physical reason for the rupture of a structural element. Because of the different material properties of reinforcing steel and concrete, a number of failure modes can occur depending on parameters such as type of cross-section, reinforcement detailing and quantities, properties of reinforcing steel, concrete compressive strength, and boundary conditions.

Paulay et al. [7] have reported failure modes for squat shear walls that are likely to fail in shear. Accordingly, diagonal tension failure can occur when a diagonal corner to corner crack forms in case of insufficient amount of horizontal reinforcement. Furthermore, monotonically loaded walls with large flexural capacities and adequate horizontal reinforcement may fail in diagonal compression. The concrete crushes in the compression zone near to the base of the wall. For cyclic loading, two sets of diagonal cracks appear, and concrete crushing can extend over the entire length of the wall due to degradation that is provoked by the load reversals.

Another reported failure mode by Paulay et al. [7] is sliding shear. Originated by flexure, a continuous horizontal crack develops along the base of the wall. Since the efficiency of aggregate interlock decreases as the number of cycle increases, the crack slip becomes important, and the wall displacements

include a significant portion due to sliding, especially at the load reversals. This phenomenon results in pinching of hysteretic loops that reduces energy dissipation.

4 Shear wall database

4.1 Static monotonic tests

Maier and Thürlimann [8] studied the behavior of barbell shaped and rectangular shear walls subjected to monotonic and cyclic loading. The specimens were tested as cantilevers that have uniformly distributed vertical reinforcement and horizontal reinforcement ratios of 0 and 1.1 %. Of particular interest for this study are specimens S4 and S9 on which constant axial load and monotonically increasing lateral load were applied. Details of these specimens are shown in Tab. 1. Specimen S9 was a replica of specimen S4 but without horizontal reinforcement. It was observed that the horizontal reinforcement had only minor influence on the peak load whereas the failure mode changed and the ultimate drift decreased. Specimen S4 failed in diagonal compression. Diagonal tension failure was reported for specimen S9.

A study of walls with concentrated boundary reinforcement was conducted by Lefas et al. [9]. One of the parameters of this study was the amount of horizontal reinforcement (0.37 %, 1.1 %) while the vertical web reinforcement ratio was equal to 2.4 %, and the specimens had 3.1 % boundary reinforcement ratio (Tab. 1). The test set-up consisted of simple cantilevers with tip load. Although the amount of horizontal reinforcement was almost reduced by a factor of three, this reduction seemed to have minor consequences on

failure mode, peak load, and achieved drift. The specimens failed in diagonal compression failure and it was concluded that the concrete compression zone contributes significantly to the overall shear strength of the wall.

4.2 Static cyclic and dynamic tests

The static-cyclic behavior of squat walls of rectangular and flanged cross-sections was addressed by Paulay et al. [7]. In the context of this paper, the specimen Wall1 is of particular interest. Its horizontal reinforcement ratio (1.6 %) was double the vertical one (0.8 %). The specimen was designed without strong boundary reinforcement (Tab. 1) and it was only subjected to lateral static-cyclic load. Axial force was not applied on this specimen. The response of this specimen was dominated by sliding shear. Significant strength loss originating from degradation of aggregate interlock occurred at displacement ductility of $\mu_\Delta = 4$. In addition, stable diagonal cracking was observed and displacements due to sliding movement yielded up to 65 % of the total displacements.

Salonikios et al. [10] carried out an experimental investigation of the validity of the design provisions of EC8 [4] for walls of height to length ratios of 1.0 and 1.5. Parameters of this test series were the web reinforcement ratios, the amount of boundary reinforcement, and the presence of diagonal reinforcement. The specimens were tested as cantilevers. Displacement ductilities up to 5.3 were observed. Furthermore, sliding shear was evident for the specimens without diagonal reinforcement which are the specimens LSW1, LSW2, and LSW3 (Tab. 1). Failure occurred due to local damage such as concrete spalling and rebar buckling at the edges of the walls. The reduction of verti-

cal and horizontal reinforcement ratios from 0.57 % to 0.28 % and boundary reinforcement from 1.7 % to 1.3 % neither affected the failure mode nor the observed drift. However, it was concluded that the lack of diagonal reinforcement anchored in the wall foundation leads to pinched hysteretic loops and diminution of energy dissipation.

Fouré [11] reported static cyclic tests of walls with height to length ratios of 0.5 that had full rotational restraint at the top and that were subjected to axial force ratios of almost 0.03. The specimens failed in diagonal tension. Horizontal reinforcement did marginally affect strength and deformation capacity while vertical reinforcement was seen to be necessary for both flexure and shear.

To investigate the unexpected good behavior of Chilean buildings in past earthquakes, Hidalgo et al. [12] studied specimens that were designed to fail in diagonal tension. Important properties of these specimen were strong vertical boundary reinforcements (6 to 11 cm^2), rotational and vertical restraining of the top section, and web reinforcement ratios between 0 and 0.38 %. Only the specimen with height to length ratios of 1.0 are reported herein (Tab. 1). Diagonal tension failure restricted the strength of the walls so that the observed strength was between 36 and 73 % of the base shear at nominal flexural strength.

Rothe [13] investigated experimentally the static-monotonic, static-cyclic, and dynamic behavior of cantilever walls with rectangular and flanged cross-sections. Of particular interest are the specimens T01, T04, T10, and T11 because of their different failure modes. The reinforcement arrangement of these specimens was the same except for specimen T04, for which the horizontal reinforcement was omitted. The specimen T01 failed because of rupture of ver-

tical rebars while diagonal tension caused failure of the specimen T04. Both specimens were tested on a shaking table. Sliding shear was observed in the static-cyclic test of T10. Specimen T11 was subjected to an axial force ratio of 0.07 and failed in diagonal compression. It was concluded that a sliding shear mode of failure would not occur in dynamic tests because dynamic sliding shear strength was considered to be significantly greater than that of the static case.

5 Experimental study

The test series which includes four specimen focuses on shear dominated response of walls that are not designed for earthquake actions. The test series investigates the deformation capacity of lightly reinforced concrete shear walls under reversed static-cyclic loading. The goal of this experimental study is to contribute to a more realistic seismic evaluation of existing shear-wall buildings that were built prior to the introduction of earthquake-resistant design recommendations into building codes. Parameters of the test series are the axial force ratio, the horizontal reinforcement ratio, and the concrete compression strength. The test program is illustrated in Fig. 1. The impact that different detailing of transversal reinforcement and lap splicing of vertical reinforcement can have on deformation capacity is not investigated in this study.

5.1 Test set-up

The specimens represent at a 1:3 scale the lower part of a shear wall of an existing building. It is assumed that a simple cantilever subjected to both con-

stant normal forces and static-cyclic lateral loads can model the behavior of a real shear wall under earthquake action in order to investigate its behavior in the laboratory. The test set-up is shown in Fig. 2. The specimen consists of three parts; the head beam through which the loads are transferred into the panel, the panel which models a shear wall, and the footing anchoring the specimen on the strong floor of the laboratory. Uplift of the footing was prevented by post-tensioned anchor rods. The head beam, panel and the footing were cast together as slab using simpler formwork than would be necessary to cast the specimen in upright position. The test program included two series, each comprised two specimens (Tab. 2).

The lateral cyclic load was applied by pushing the head beam with two actuators of 200 kN maximum force that were operated alternately. Two post-tensioning bars of 12 mm diameter were used to subject the specimens to axial loading. The bars were placed at mid-length of the specimens at both sides of the panel. Circular ducts of 50 mm diameter in both the footing and the head beam prevented contribution of these bars to the lateral stiffness of the specimen. Anchoring was provided to the post-tensioning bars by screws and washers that were placed in a recess of the footing and above the head beam. Before the static-cyclic test, the bars alternately were post-tensioned in small increments up to the target force by the help of a hydraulic jack. Because the vertical post-tensioning force could not maintained on a constant level, railcar springs between the head beam and the anchor of the post-tensioning bars allowed to reduce the stiffness of the post-tensioning system. Thus, the uplift of the head beam due to rocking of the panel resulted in less increase of axial load.

The reinforcement of the specimens is illustrated in Fig. 3. Mild steel rebars

of 6 mm diameter form the vertical reinforcement for all specimens and the horizontal reinforcement of specimen M1 while cold formed rebars of 4 mm diameter were used for the horizontal reinforcement of specimens M3 and M4. Mean values of the mechanical properties of the rebars are shown in Tab. 3. The vertical reinforcement is enclosed by the horizontal reinforcement in the form of stirrups with end hooks of 135° that are anchored in the core concrete. The openings of the stirrups are staggered along the wall height. Rebars of 12 mm diameter were used for the reinforcement of the head beam and the footing.

5.2 Testing procedure and loading history

The instrumentation of the specimens with force transducers, displacement transducers and deformeter targets allowed to monitor loads, in-plane displacements and strains on the concrete surface, respectively. The load was quasi-statically applied in small increments up to a target displacement or a target force. At this point the displacement was kept constant in order to capture high-resolution images, measure crack widths and record strains on the surface. The force decreased during this time by 10% to 15 %. Finally, the specimen was gradually unloaded.

Force and displacement controlled loading histories were applied in order to simulate seismic actions by reversed static-cyclic loading. Specimens M1 and M2 were cycled at 25, 50, 100, 150 kN base shear and nominal axial force of 136 kN (Fig. 4). Two cycles were applied at each level of base shear. The specimens were then subjected to three cycles at 200 kN base shear which was near to the base shear at nominal flexural strength. Because of the limited load

capacity of the actuators, further increase of base shear was not possible. The vertical post-tensioning force was then decreased to 106 kN and the specimen was subjected to two cycles of lateral loading. Subsequently, the vertical post-tensioning force was reduced to 86 kN and the specimen was cycled up to failure. Specimens M3 and M4 were subjected to constant nominal axial forces of 136 and 76 kN, respectively (Fig. 5). The cyclic loading regime of these specimen included load increments of 25 kN up to 75 % of the base shear at nominal flexural strength and displacement increments corresponding to the top lateral displacement at 75 % base shear at nominal flexural strength.

5.3 Test results

The force-displacement relationships are shown in Fig. 6. In addition to the observed responses, the plots include a bilinear approximation of the load-displacement curve and the corresponding values of ductility and drift. The observed failure modes are also indicated in Fig. 6. The bilinear approximation was determined by extrapolating the observed top lateral displacement at first yield up to the nominal flexural strength ([15],[16]). Both first yield and nominal flexural strength are derived from moment-curvature relationships that were computed with the material properties shown in Tabs. 2 and 3. The assumptions for these calculations include elastic-perfectly plastic and parabolic-rectangular stress-strain relationships for reinforcing steel and concrete, respectively. Depending on the specimen configuration, yielding of the outermost rebars occurred between 76 % to 82 % of the nominal flexural strength.

All specimens approximately developed the nominal flexural strength and

hence, the observed maximum base shear was controlled by flexure, and not by premature shear failure. The observed maximum base shear of specimen M3 is even greater than the base shear at nominal flexural strength. The specimens failed due to increase of applied displacements. The ultimate displacement was restricted by shear failure or flexural failure, depending on the axial force ratio that was applied on the specimen.

For specimen M1, cracking localized at the base of the wall. Almost linear-elastic behavior was observed up to a magnitude of base shear of 150 kN which is closed to the predicted yielding of the outermost rebars. Then the slope of the response curve changes significantly. Displacements up to 3.5 mm and axial force of 136 kN resulted in a number of small inclined cracks that formed in a zone of 40 mm width between the footing and the first stirrup. The inclined crack (Fig. 7) occurred at 3.5 mm top lateral displacement. Reduction of axial force resulted in diminution of stiffness. The small cracks near to the base interconnected with increase of displacements and sliding movements in these cracks contributed substantially to the top lateral displacements. The rupture of the outermost rebars was observed at a top lateral displacement of 16.5 mm. In addition, the vertical force was not constant during the test. It varied between 136 and 146 kN, 106 and 122 kN, 80 and 106 kN for nominal axial forces of 136 kN, 106 kN, and 86 kN, respectively.

During the test of specimen M2, residual displacements were already observed at a value of base shear equal to 150 kN. As for specimen M1, the slope of the response curve diminished at the predicted yield of the outermost rebars. Reduce in stiffness due to both diminution of axial force and increasing number of cycles was also observed. However, at the toes of the wall the cracking extended up to one third of the wall height. A continuous base crack did not

form. The concrete cover at the edges spalled at 5 mm displacement. The movement of the wall consisted then of sliding at the load reversal and subsequent rocking. The test was halted at 15 mm top lateral displacement because the vertical displacements exceeded the capacity of the test set-up. During the test of specimen M2, the vertical post-tensioning force varied between 136 and 144 kN, 106 and 112 kN, 75 and 108 kN for nominal axial forces of 136 kN, 106 kN, and 86 kN, respectively. The maximum axial force was observed at the peak of the half-cycles.

Specimen M3 developed its maximum base shear of 176 kN at 3.2 mm top lateral displacement. At this time, cracking was limited to the lowest third of the wall. Small vertical cracks occurred at the base of the wall near its edges. Increasing the displacement to 7 mm resulted in the formation of a diagonal corner to corner crack (Fig. 7). Due to the cracking, the restoring force decreased by nearly 15 %. Moreover, both spalling of concrete cover at the wall toe and buckling of the outermost rebars was observed at the begining of the cycle in which the diagonal crack formed. Despite the occurrence of the diagonal crack, the shear capacity of the specimen was yet greater than 80 % of the base shear at nominal flexural strength. The second diagonal crack occurred at 8.7 mm top lateral displacement resulting in a drop of the restoring force by 30 %. In the lowest quarter of the wall, the vertical strain at the edge increased by 6 mm/m. The crack pattern at this stage is shown in Fig. 7. Significant loss of shear capacity was observed in the subsequent cycles. Fig. 8 shows the edge of specimen M3 at 10 mm top lateral displacement, after the second diagonal crack occurred. Sudden concrete crushing along the base of the wall terminated the test of specimen M3.

The maximum shear capacity of specimen M4 was observed at 2.8 mm top

lateral displacement (Tab. 4). The crack pattern at maximum base shear was very similar to that of specimen M3 but the hysteretic loops of specimen M4 are more pinched than those of the other specimens (Fig. 6). Spalling of the concrete cover at the wall toes was observed at 4.9 mm top lateral displacement. The outermost vertical rebars buckled at the displacement level of 7 mm. Nevertheless, the shear capacity at the subsequent displacement level of 9 mm was almost equal to the base shear at nominal flexural strength. The shear capacity decreased in the second cycle at this displacement level by 13 % while in previous cycles up to 7.5 % loss of shear capacity due to repeated loading was observed. Further increase in displacement led to the failure of both the vertical rebars in tension and concrete in compression at the wall edges. The maximum top lateral displacement yielded 12.5 mm.

5.4 Discussion of test results

Strength, top lateral displacements and achieved ductility are shown in Tab. 4. Failure of the specimen is assumed to occur when the shear capacity falls below 80 % of the shear capacity that was observed in the second cycle at the top lateral displacement corresponding to the maximum observed base shear. The ductility is then computed from the ultimate displacement and the extrapolated displacement at first yield.

The drift capacity of all specimens is greater than or equal to 0.8 %. The test results of specimens M2, M3, and M4 indicate that the higher the axial force ratio, the lesser is the drift capacity. For specimen M1, the smallest drift capacity was observed due to concentration of deformations in the base crack. This concentration depends on concrete quality, the axial force ratio and

the detailing of horizontal reinforcement. Although significant degradation of shear capacity was observed, the vertical load bearing capacity of the wall was maintained until the end of the test.

The concentration of deformation in the base crack reduces the effect of aggregate interlock because of significant crack widths. Thus, the compressed part of the wall contributes almost solely to the transfer of shear forces to the footing. Taking into account the low ratio of vertical reinforcement, inclined tensile strains that can cause inclined cracking are less important for lower axial force ratios and diagonal tensile failure is prevented. This is evident when comparing the behavior of specimens M3 and M4.

Due to sliding movements in regions of the interconnected cracks at the base of the wall, residual displacements increase as the axial force ratio decreases. The tested specimens had no construction joint between the footing and the wall. A construction joint can result in a reduction of the sliding shear strength, and hence the sliding shear becomes more important.

Specimens M1 and M2 were cycled with maximum base shear of 200 kN. This load magnitude yields a nominal shear stress ratio ($v = \tau_{max}/\sqrt{f'_c}$) of 0.29. The test results of specimens M1 and M2 indicate that tensile strength of concrete plays an important role in shear transfer. Vertical reinforcement ratios of 0.3 % and axial force ratios less than 3 % are probably not sufficient to develop shear forces that overcome the tensile strength in the wall. Thus, horizontal reinforcement would not be required since cracking is restricted at the base of the wall.

6 Comparison of tests with database

The experimental study and shear wall tests from the literature (Tab. 1) are compared in terms of nominal shear stress ratio and drift. In Figure 9 the nominal shear stress ratio is plotted against drift. The nominal shear stress ratio was derived from maximum base shear while the drift was calculated from the ultimate top lateral displacements. The designations of the specimens in the plot refer to Tabs. 1 and 2. Specimen M3 shows good performance when compared with the specimens LSW3 [10], and S4 [8]. All four specimens were subjected to axial force ratios of nearly 7 %. The nominal shear stress ratios are between 0.45 and 0.6. Although these specimen have a similar drift capacity of 1.2 %, three different failure modes were observed that are closely linked to the reinforcement arrangement.

Relative displacements were measured between targets glued on the concrete surface of specimens M1, M2, M3, and M4. Strain fields derived from these data substantiate the observations on failure modes. Significant strains concentrations are observed in the lower fourth of specimens M1, M2, and M4 while the results for specimen M3 show lesser strain concentrations and deformations of the upper part of the panel. Only the results of specimen M3 are compared with test results form the literature since the strain fields of the other specimens are influenced by both the degradation of crack interface and sliding. Strains are also available for specimens S4 and S9 [8]. It is found that in the compressed region of the wall both compressive and tensile principal strains of specimen M3 are greater than that of specimens S4 and S9. Thus, both diagonal tension failure and diagonal compression failure damage the concrete compression zone by straining.

Although the horizontal reinforcement ratios of specimens M1, M2, M3, and M4 are similar to those of the specimens tested by Fouré [11] and to specimens studied by Hidalgo et al. [12], the failure modes and deformation capacities are substantially different. Thus, other parameters such as the amount of boundary reinforcement, the boundary conditions at the top of the wall, and the shear span ratio influence both failure modes and deformation capacity. Lower shear span ratios, stronger boundary reinforcement and restrained top sections lead to less deformation capacity and diagonal tension failure.

7 Conclusions

Static-cyclic tests of lightly reinforced concrete wall specimen that model shear walls of existing buildings in Switzerland indicate other failure modes and drift capacity than one would expect from data available in the literature. The flexural capacity of the specimens limited the maximum observed base shear whereas shear related failure modes such as sliding, diagonal compression, and diagonal tension restricted the deformation capacity of the specimens. The variation of concrete compressive strength and of axial force ratio lead to crack patterns that are substantially different. It was further observed that damage due to reversed static-cyclic loading accumulates near the base of the wall thereby degrading the concrete in sliding, compression, and tensile straining.

The study also showed that shear walls that were only designed for gravity loads can have drift capacity greater than 1 %. The comparison with other tests from the literature shows that for squat walls, the drift capacity depends on axial force ratio, vertical reinforcement arrangement, and degree of restraining

at the top of the wall. Cantilever shear walls without rotation restraints are less susceptible to brittle shear failure than walls with fixed top ends.

8 Acknowledgements

The research was partially founded by the Swiss National Science Foundation. The writers acknowledge gratefully the contributions of CREALP (Sion) and Stahl Gerlafingen for the experimental part of the study. Comments and suggestions from anonymous reviewers are deeply appreciated.

A Glossary

A	: Concrete gross-section.
a	: Shear span ratio (Lever arm of base shear divided by wall length).
f'_c	: Mean concrete compressive strength on cylinder.
f_y	: Mean yield strength of rebars.
f_u	: Mean tensile strength of rebars.
F_y	: Base shear at nominal flexural strength.
h_F	: Wall height.
h/l	: Geometric slenderness ratio.
l_w	: Wall length.
N	: Axial force.
t	: Panel thickness.
V_{max}	: Maximum base shear.
V_u	: Ultimate base shear.
v	: Nominal shear stress ratio.
ϵ_u	: Uniform Strain. Maximum uniformly distributed strain before necking occurs.
ϵ_y	: Yield strain.
Δ	: Top lateral displacement.
Δ_{max}	: Top lateral displacement at maximum base shear.
Δ_u	: Top lateral displacement at failure.
μ_Δ	: Displacement ductility.
ρ_h	: Geometric reinforcement ratio in horizontal direction.
ρ_v	: Geometric reinforcement ratio in vertical direction.
ρ_e	: Geometric reinforcement ratio of vertical boundary reinforcement.
τ_{max}	: Maximum shear stress, computed from maximum base shear divided by concrete gross-section.
τ_u	: Ultimate shear stress, computed from ultimate base shear divided by concrete gross-section.

References

[1] Priestley M J N. Displacement-based seismic assessment of reinforced concrete buildings. Journal of Earthquake Engineering 1997;1(1):157-192.

[2] Fintel M. Performance of buildings with Shear Walls in Earthquakes of the Last Thirty Years. PCI Journal 1995;40(3):62-80.

[3] Pellissier V. Evaluation de stratégies pour la gestion du risque sismique du bâtiment. PhD-thesis. Lausanne: Ecole polytechnique fédérale; 2004.

[4] Eurocode 8. Design provisions for earthquake resistance of structures - Part 1-3: General rules - Specific rules for various materials and elements. Bruxelles: CEN - European Comittee for Standardization; 1995.

[5] SIA262. Concrete structures, Zurich: Swiss Society of Engineers and Architects; 2004.

[6] Peter K. Erdbebenüberprüfung bestehender Stahlbetongebäude. PhD-thesis. Lausanne: Ecole polytechnique fédérale; 2000.

[7] Paulay T, Priestley M J N, Singe A J. Ductility in Earthquake Resisting Squat Shearwalls. ACI Journal 1982;79(4):257-269.

[8] Maier J, Thürlimann B. Bruchversuche an Stahlbetonscheiben. IBK Bericht 8003-1. Zürich: ETH; 1985.

[9] Lefas I, Kotsovos M, Ambraseys N. Behavior of Reinforced Concrete Structural Walls: Strength, Deformation Characteristics, and Failure Mechanisms. ACI Structural Journal 1990;87(1):23-31.

[10] Salonikios T, Kappos A, Tegos A, Penelis G. Cyclic load behaviour of low slenderness reinforced concrete walls: design basis and test results. ACI Structural Journal 1999;96(4):649-660.

[11] Fouré B. Un programme d'essais des murs de contreventement. In: Colloquium AFPS-SECED Experimental Methods in Earthquake Engineering and Structural Dynamics. Saint-Rémy-lès-Chevreuse: AFPS - Association Francaise du Genie Parasismique; 1993.

[12] Hidalgo P A, Ledezma C, Jordan R M. Seismic behavior of squat reinforced concrete shear walls. Earthquake Spectra 2002;18(2):287-308.

[13] Rothe D. Untersuchungen zum nichtlinearen Verhalten von Stahlbetonwandscheiben unter Erdbebenbeanspruchung. Reihe 4 Nr. 117 VDI-Fortschrittsberichte. Düsseldorf: VDI-Verlag; 1992.

[14] Greifenhagen C, Lestuzzi P, Papas D. Static-cyclic tests on reinforced concrete shear walls with low reinforcement ratios. Rapport IMAC Nr. 4. Lausanne: Ecole polytechnique fédérale; 2005 (http://imac.epfl.ch/Team/Greif/reportIMACno4.pdf).

[15] Priestley M J N, Kowalsky M J. Aspects of Drift and Ductility Capacity of rectangular cantilever structural Walls. Bulletin of the New Zealand National Society for Earthquake Engineering 1998;31(2):73-85.

[16] Dazio A, Wenk T, Bachmann H. Versuche an Stahlbetonwänden unter zyklisch-statischer Einwirkung. IBK Bericht 239. Zürich: ETH; 1999.

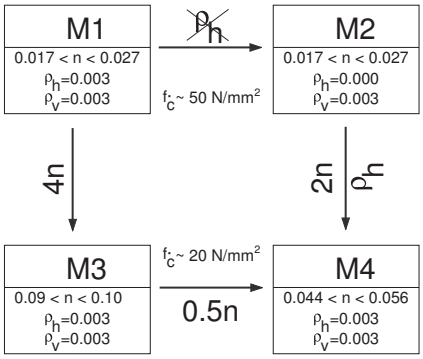

Fig. 1. Test program [14].

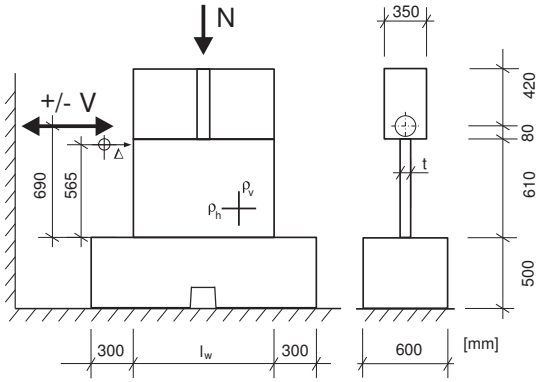

Fig. 2. Set-up of static-cyclic tests [14].

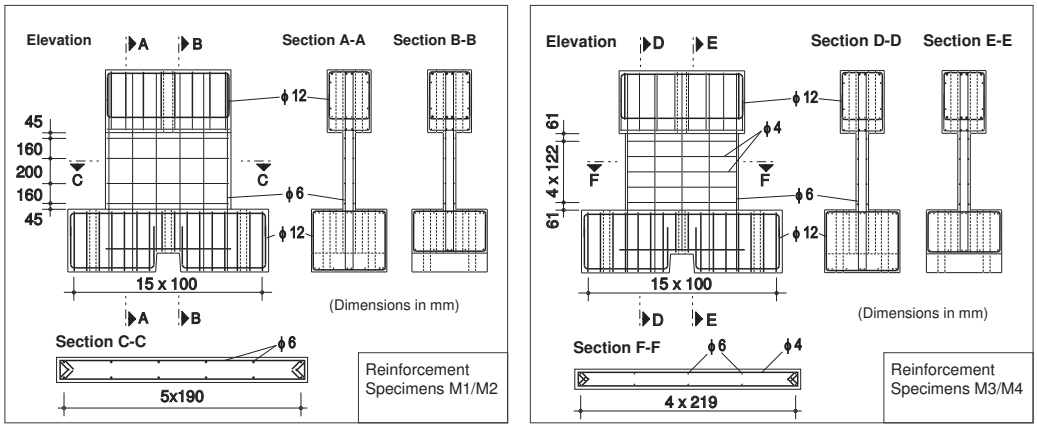

Fig. 3. Reinforcement of specimens.

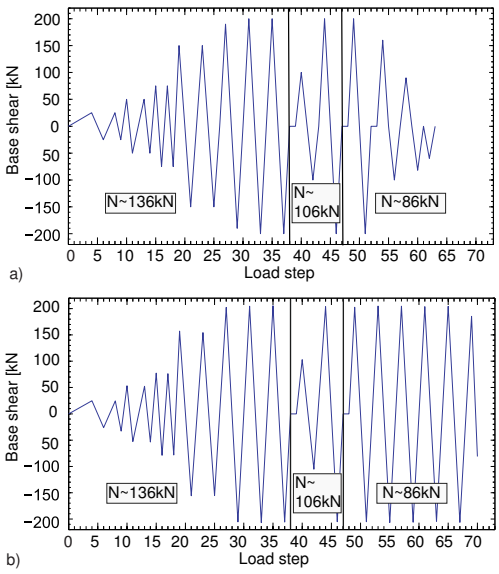

Fig. 4. Loading history of specimens, a) M1, b) M2.

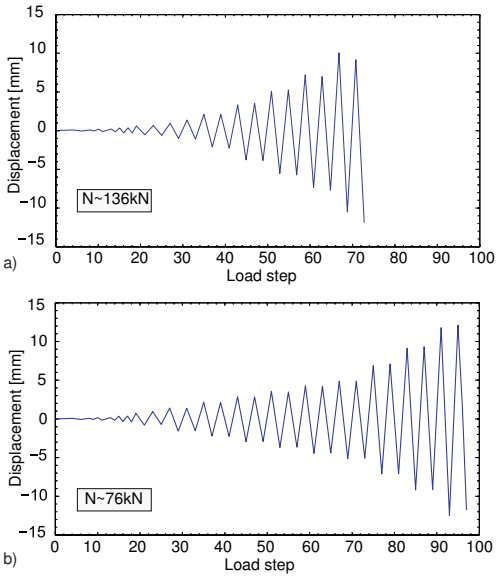

Fig. 5. Loading history of specimens, a) M3, b) M4.

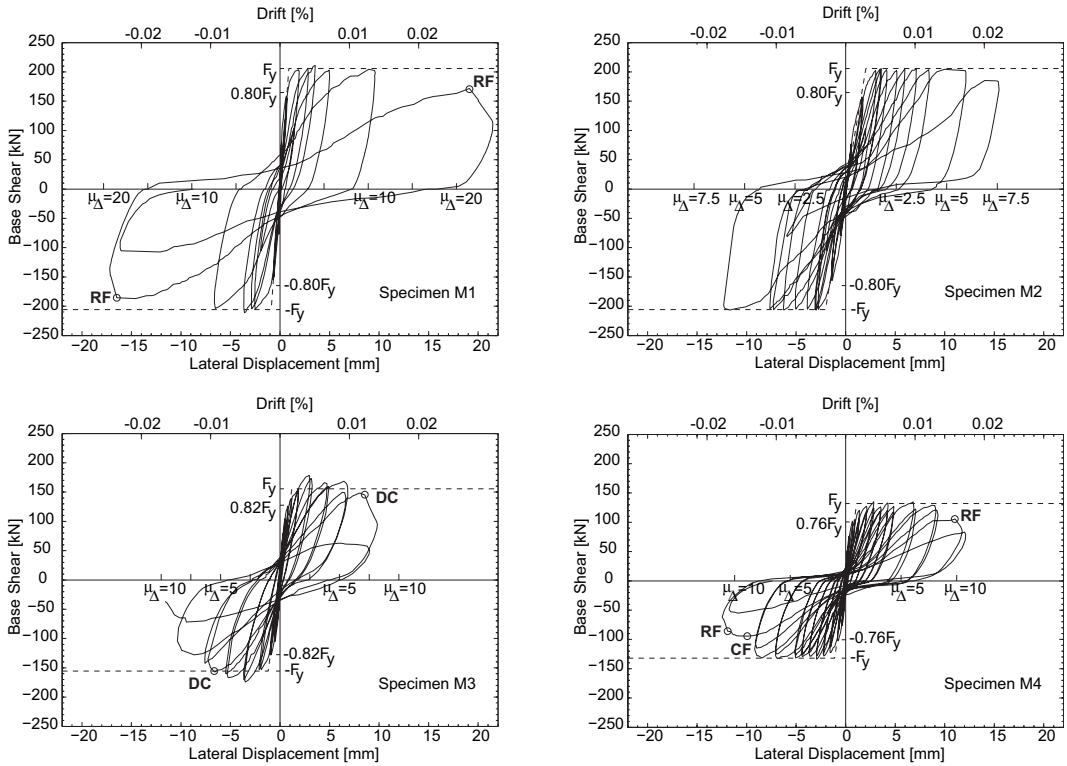

Fig. 6. Force-displacement relationships observed in static-cyclic tests (RF-Failure of vertical reinforcement, DC-Diagonal cracking, CF-Concrete compression failure)

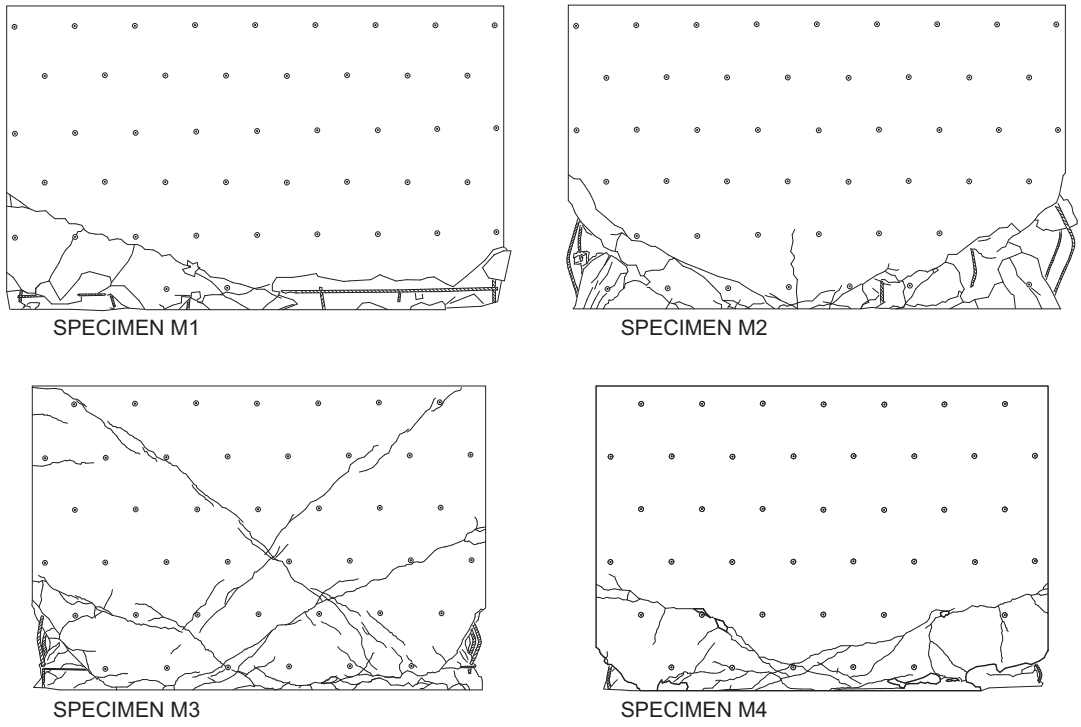

Fig. 7. Final crack patterns.

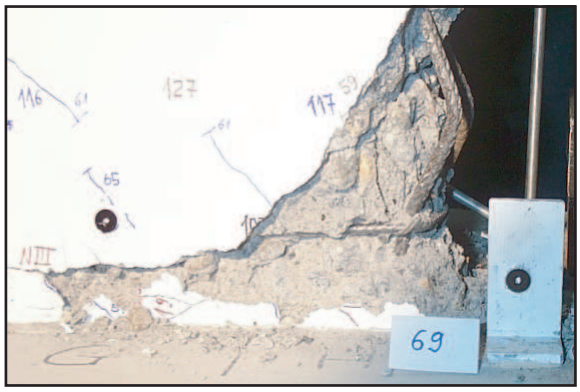

Fig. 8. Detail of specimen M3 at 10 mm top lateral displacement.

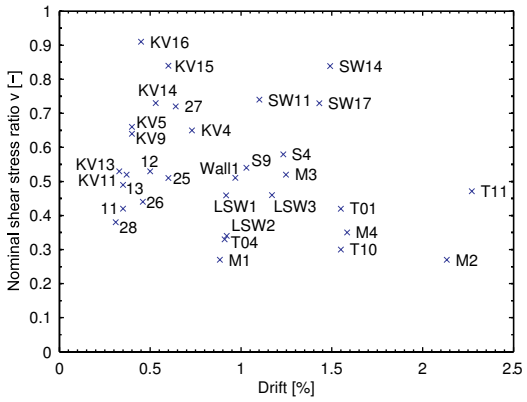

Fig. 9. Summary of shear wall tests.

Table 1

Tests of shear walls up to slenderness ratios of 1.5. (Applied loadings: mon - static-monotonic, dyn - dynamic, st - static-cyclic.)

Ref.	Specim.	Load	h_F [m]	l_w [m]	t [m]	h/l [-]	ρ_h [%]	ρ_v [%]	ρ_e [%]	f'_c [MPa]	a [-]	n [%]
[8]	S4	mon	1.20	1.18	0.10	1.02	1.03	1.05	1.05	32.90	1.12	6.7
	S9	mon	1.20	1.18	0.10	1.02	0.00	1.05	1.05	29.20	1.12	7.5
[9]	SW11	mon	0.75	0.75	0.07	1.00	1.10	2.40	3.10	44.46	1.10	-
	SW14	mon	0.75	0.75	0.07	1.00	1.10	2.40	3.10	35.79	1.10	-
	SW17	mon	0.75	0.75	0.07	1.00	0.37	2.40	3.10	41.06	1.10	-
[13]	T01	dyn	1.10	0.80	0.08	1.38	0.47	0.71	1.42	24.31	1.50	-
	T04	dyn	1.10	0.80	0.08	1.38	0.00	0.71	1.42	28.80	1.50	-
	T10	st	1.10	0.80	0.08	1.38	0.47	0.71	1.42	33.57	1.50	-
	T11	st	1.10	0.80	0.08	1.38	0.47	0.71	1.42	26.86	1.50	7.0
[7]	Wall1	st	1.50	3.00	0.10	0.50	1.60	0.81	0.85	27.20	0.57	-
[10]	LSW1	st	1.20	1.20	0.10	1.00	0.57	0.57	1.70	22.20	1.09	-
	LSW2	st	1.20	1.20	0.10	1.00	0.28	0.28	1.30	21.60	1.09	-
	LSW3	st	1.20	1.20	0.10	1.00	0.28	0.28	1.30	23.90	1.09	7.0
[12]	11	st	1.40	1.40	0.10	1.00	0.13	0.26	(8.0) [1]	16.30	0.50	-
	12	st	1.40	1.40	0.10	1.00	0.26	0.13	(8.0) [1]	17.00	0.50	-
	13	st	1.40	1.40	0.10	1.00	0.26	0.26	(8.0) [1]	18.10	0.50	-
	25	st	1.40	1.40	0.10	1.00	0.00	0.00	(6.0) [1]	23.90	0.50	-
	26	st	1.40	1.40	0.10	1.00	0.00	0.00	(6.0) [1]	17.70	0.50	-
	27	st	1.40	1.40	0.10	1.00	0.25	0.00	(9.1) [1]	23.90	0.50	-
	28	st	1.40	1.40	0.10	1.00	0.00	0.25	(6.0) [1]	23.30	0.50	-
[11]	KV11	st	0.75	1.50	0.10	0.50	0.12	0.12	1.07	30.20	0.25	1.7
	KV4	st	0.75	1.50	0.10	0.50	0.20	0.20	1.13	32.50	0.25	1.5
	KV5	st	0.75	1.50	0.10	0.50	0.28	0.28	1.57	30.20	0.25	1.7
	KV13	st	0.75	1.50	0.10	0.50	0.12	0.12	1.07	15.60	0.25	3.2
	KV9	st	0.75	1.50	0.10	0.50	0.20	0.20	1.13	16.60	0.25	3.0
	KV14	st	0.75	1.50	0.10	0.50	0.28	0.28	1.57	16.10	0.25	3.1
	KV15	st	0.75	1.50	0.10	0.50	0.39	0.39	2.01	27.10	0.25	1.8
	KV16	st	0.75	1.50	0.10	0.50	0.68	0.68	3.14	28.20	0.25	1.8

[1] Units: cm^2

Table 2

Characteristics of specimens

Specimen	l_w [mm]	t [mm]	M/V [-]	ρ_v [%]	ρ_h [%]	f'_c [MPa]	n [%]
M1	1000	100	0.69	0.3	0.3	50.7	1.7 .. 2.7
M2	1000	100	0.69	0.3	0.0	51.0	1.7 .. 2.7
M3	900	80	0.69	0.3	0.3	20.1	4.4 .. 5.6
M4	900	80	0.69	0.3	0.3	24.4	9.0 .. 10.0

Table 3

Properties of reinforcement

Type	f_y [MPa]	f_u [MPa]	ϵ_y [mm/m]	ϵ_u [cm/m]	$\frac{f_u}{f_y}$ [-]
4 mm cold formed bar	745	800	3.71	2.91	1.07
6 mm mild steel bar	504	634	2.85	11.05	1.26

Table 4

Test results: Strength, top lateral displacements and ductility.

Specim.	N [kN]	n [-]	V_{max} [kN]	V_u [kN]	τ_{max} $[MPa]$	τ_u $[MPa]$	Δ_{max} [mm]	Δ_u [mm]	$\frac{\Delta_u}{h_F}$ [%]	μ_Δ [-]
M1	-135	0.03	204	140	2.04	1.40	1.88	5.00	0.89	5.6
M2	-140	0.03	203	156	2.03	1.56	2.88	12.13	2.15	5.9
M3	-140	0.10	176	134	2.44	1.86	3.2	7.07	1.25	5.8
M4	-87	0.05	135	101	1.88	1.40	2.8	9.00	1.59	8.0